In situ TEM Investigation on Fatigue Behavior of Single ZnO Wires under High-Cycle Strain.

ARTICLE *in* NANO LETTERS · JANUARY 2014

Impact Factor: 13.59 · DOI: 10.1021/nl403426c · Source: PubMed

NANO LETTERS

Letter

pubs.acs.org/NanoLett

In Situ Transmission Electron Microscopy Investigation on Fatigue Behavior of Single ZnO Wires under High-Cycle Strain

Peifeng Li,[†,#] Qingliang Liao,[†,#] Shize Yang,[‡] Xuedong Bai,[‡] Yunhua Huang,[†] Xiaoqin Yan,[†] Zheng Zhang,[†] Shuo Liu,[†] Pei Lin,[†] Zhuo Kang,[†] and Yue Zhang*[,†]

[†]State Key Laboratory for Advanced Metals and Materials, School of Materials Science and Engineering, Key Laboratory of New Energy Materials and Technologies, University of Science and Technology Beijing, Beijing 100083, People's Republic of China

[‡]National Laboratory for Condensed Matter Physics, Institute of Physics, Chinese Academy of Sciences, Beijing, 100190, People's Republic of China

ABSTRACT: The fatigue behavior of ZnO nanowires (NWs) and microwires was systematically investigated with in situ transmission electron microscopy electromechanical resonance method. The elastic modulus and mechanical quality factors of ZnO wires were obtained. No damage or failure was found in the intact ZnO wires after resonance for about 10^8−10^9 cycles, while the damaged ZnO NW under electron beam (e-beam) irradiation fractured after resonance for seconds. The research results will provide a useful guide for designing, fabricating, and optimizing electromechanical nanodevices based on ZnO nanomaterials, as well as future applications.

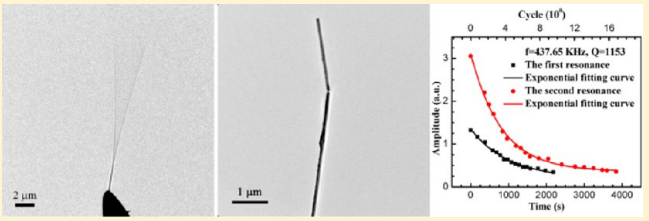

KEYWORDS: *ZnO wires, in situ TEM, electromechanical resonance, fatigue behavior, elastic modulus*

Because of the unique semiconducting and piezoelectric properties, ZnO nanomaterials[1−5] are considered as one of the most promising candidates for the fabrication of electromechanical devices, including nanogenerators,[6,7] piezoelectric gated diode and transistors,[8−10] and flexible piezoelectric strain sensors.[11] These devices will be subjected to external forces and large deformations. Therefore, it is important to investigate the mechanical properties and service behavior of ZnO nanomaterials, which are critical for the device fabrication and performance enhancement.

Recently, some mechanical properties and corresponding damage or failure phenomena of ZnO nanomaterials have been investigated by some researchers.[12−22] Zhu et al. obtained large strain of ZnO nanowires (NWs) up to 4−7% before the final elastic fracture induced by the atomic force microscopy (AFM) tip.[12] For small diameter ZnO NWs (~18 nm), Boland et al. found the brittle fracture and the ultimate strength approached the value of 7.00 GPa.[19] Xu et al. carried out a systematic experimental and theoretical investigation on the elastic and failure properties of ZnO NWs under different loading modes via in situ scanning electron microscopy (SEM) test, indicating that fracture strain and strength of ZnO NWs increased as the NW diameter decreased.[14] Additionally, the mechanical and electromechanical damage and failure phenomena of ZnO NWs were observed using nanomanipulation and C-AFM system by Zhang's group,[21,22] while the fatigue behavior under high-cycle strain is rarely reported.[23] Actually, the fatigue damage or failure occurring under high-cyclic loading conditions is a commonly encountered mode of damage or failure in nanomaterials that determines the stability and lifetime of nanodevices.

In this Letter, we study the fatigue behavior of single ZnO wires under high-cycle strain for about 10^9 cycles with in situ transmission electron microscopy (TEM) electromechanical resonance method. The elastic modulus and resonance quality factor of ZnO wires are obtained, and the damping effect as function of the resonance time and cycles are deeply discussed. The research results will provide a useful guide for designing, fabricating, and optimizing electromechanical nanodevices based on ZnO nanomaterials, as well as future applications.

Results and Discussion. The typical TEM images and corresponding selected area electron diffraction (SAED) pattern of the ZnO NW are shown in Figure 1. The TEM images indicate that the ZnO NW has uniform diameter, and the SAED pattern implies that the ZnO NW is single crystal and grows along [0001] direction.

The schematic of the electromechanical resonance test is exhibited in Figure 2a. The images of ZnO NW in stationary and resonance states are shown in Figure 2b,c, respectively. Figure 2c indicates excellent resonance symmetry that reveals that the vibrating plane of the ZnO NW is aligned perpendicular to the e-beam.

Because of the difference in the surface work functions between the ZnO wire and the counter Au electrode, a static charge Q_0 exists at the tip of the ZnO to balance this potential difference even at zero applied voltage.[19] The magnitude of Q_0 is proportional to the difference between work functions of the Au electrode and the ZnO tip

Received: September 13, 2013
Revised: December 22, 2013
Published: January 1, 2014

$$Q_0 = \alpha(W_{Au} - W_{ZnO}) \quad (1)$$

where α is related to the geometry and distance between the ZnO and the electrode.

As mentioned in previous work, an oscillating voltage with tunable frequency was applied to produce electromechanical resonance of the ZnO NW.[24] In this case, an oscillating voltage $V_{ac} \cos 2\pi ft$ is applied on the ZnO wire, as shown in Figure 2a, where f is the frequency and V_{ac} is the applied voltage of alternating current. The total induced charge on the ZnO wire is

$$Q = Q_0 + \alpha e V_{ac} \cos 2\pi ft \quad (2)$$

The force acting on the ZnO wire is proportional to the square of the total charge on the ZnO wire

$$F = \beta(Q_0 + \alpha e V_{ac} \cos 2\pi ft)^2 = \alpha^2\beta\left\{\left[(W_{Au} - W_{ZnO}) + \frac{e^2 V_{ac}^{\ 2}}{2}\right] + 2eV_{ac}(W_{Au} - W_{ZnO})\cos 2\pi ft + \frac{e^2 V_{ac}^{\ 2}}{2\cos 4\pi ft}\right\} \quad (3)$$

where β is a proportional constant. In the above equation, the first term is constant and it causes a static deflection of the ZnO wire; the second term is a linear term, and the resonance occurs if the applied frequency f approaches the intrinsic mechanical resonance frequency f_0 of the ZnO wire; and the last term is the second harmonics. For the linear term, the resonance amplitude A of the ZnO wire is proportional to $V_{ac}(W_{Au} - W_{ZnO})$. And the resonance amplitude A is approximately proportional to the applied voltage of alternating current V_{ac}.[24,25]

A ZnO NW with l_1 = 9735 nm and d_1 = 148 nm and another ZnO NW with l_2 = 9912 nm and d_2 = 177 nm are used for fatigue tests. Each ZnO NW is tested twice with different oscillation amplitudes (Figure 3a–d) in order to ensure the reliability and repeatability of the resonance experiments. To investigate the fatigue behavior of the ZnO NWs, an oscillating voltage of alternating current with tunable frequency is applied on the ZnO NW so that the resonance can be induced by changing the frequency.[26] The amplitude (defined as the distance between the two limited positions) can be controlled by the applied voltage of alternating current. The oscillation amplitudes of the first ZnO NW are A_{11} = 2000 nm, corresponding to a vibration angle of 14° ($\varepsilon_{11} = d_1/2R_{11}$ = 148/(2 × 11583) = 0.64%, R_{11} is the curvature radius of the first resonance, and R_{12}, R_{21}, R_{22} are also the curvature radius)[1,27] under V_{11} = 2 V (−2 to 2 V, the peak voltage difference is 4 V, and the same as V_{12}, V_{21}, and V_{22}) for the first resonance, and A_{12} = 2340 nm, corresponding to a vibration angle of 17° ($\varepsilon_{12} = d_1/2R_{12}$ = 148/(2 × 10175) = 0.73%) under V_{12} = 2.5 V for the second resonance, respectively. The oscillation amplitudes of the second ZnO NW are A_{21} = 1319 nm, corresponding to a vibration angle of 10° ($\varepsilon_{21} = d_2/2R_{21}$ = 177/(2 × 11109) = 0.80%) under V_{21} = 1.5 V for the first resonance, and A_{22} = 3064 nm, corresponding to a vibration angle of 23° ($\varepsilon_{22} = d_2/2R_{22}$ = 177/(2 × 7708) = 1.15%) under V_{22} = 3 V for the second resonance, respectively. Figure 3e shows the relationship between the amplitude and

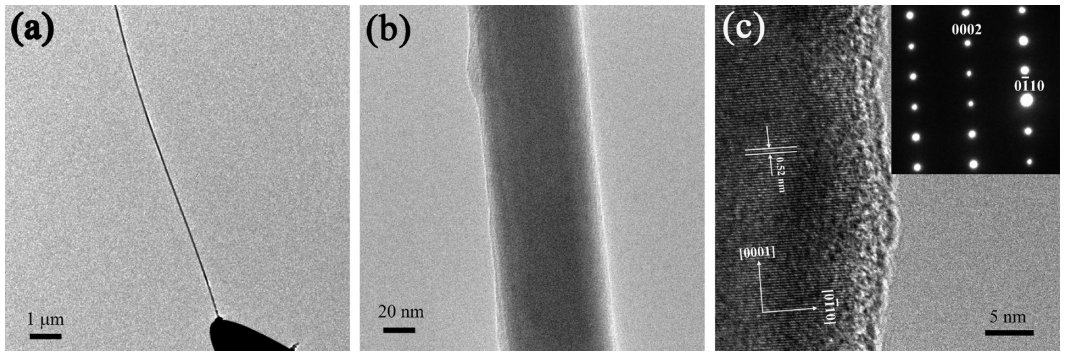

Figure 1. TEM images of the ZnO NW used in the electromechanical resonance experiment: (a) low magnification and (b) high magnification. (c) The HRTEM image and corresponding SAED pattern shown in the inset.

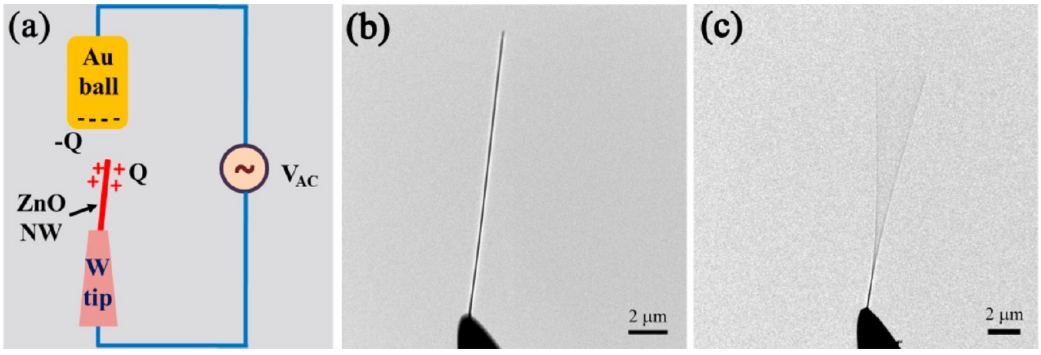

Figure 2. (a) Schematic of the experimental approach for resonance tests of the single ZnO NW. (b,c) The images of the ZnO NW in stationary and resonance state in TEM, respectively.

dx.doi.org/10.1021/nl403426c | Nano Lett. 2014, 14, 480–485

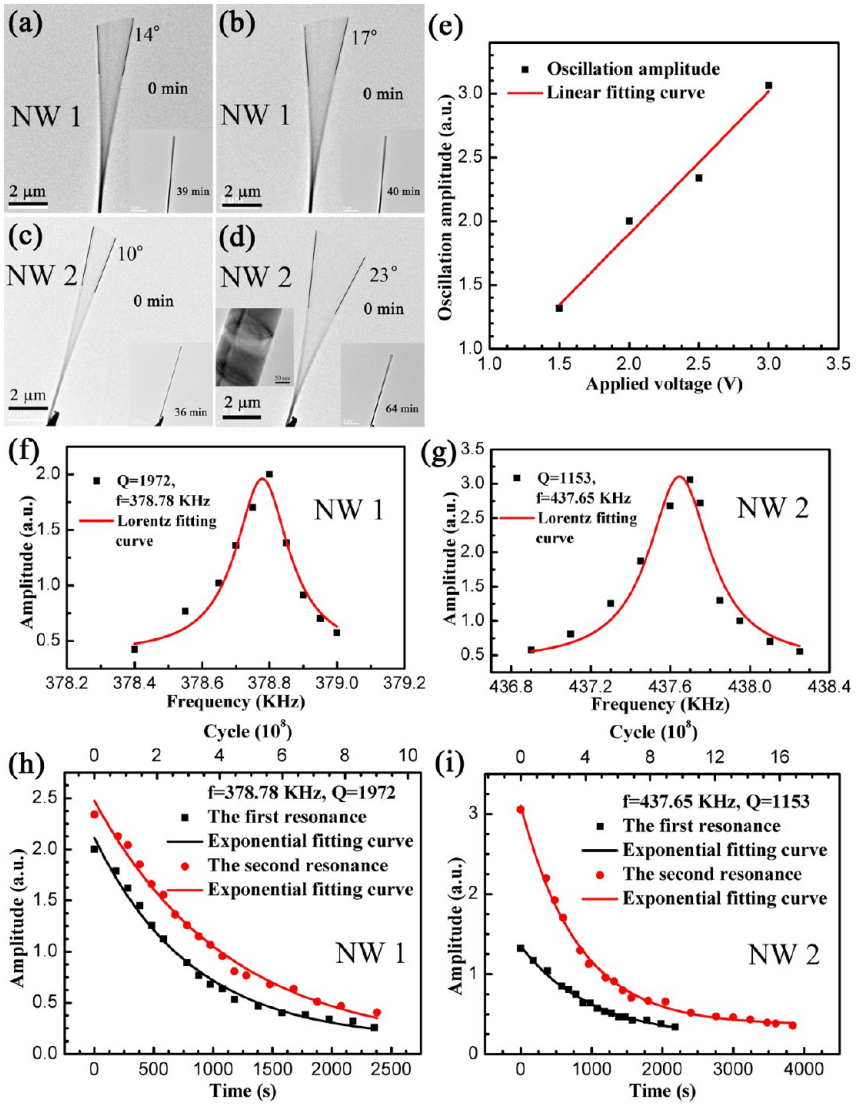

Figure 3. In situ TEM resonance images of the ZnO NW with d_1 = 148 nm: (a) A_{11} = 2.000 μm and (b) A_{12} = 2.340 μm. In situ TEM resonance images of the ZnO NW with d_2 = 177 nm: (c) A_{21} = 1.319 μm and (d) A_{22} = 3.064 μm. (e) Oscillation amplitudes of the two ZnO NWs with approximate lengths (9735 and 9912 nm, respectively) as function of the applied voltage of alternating current V_{ac} that shows a linear dependence. (f,g) The measured fwhm of the resonance peaks from the two ZnO NWs, respectively. (h,i) The amplitude changes of the ZnO NWs with time and cycles increasing.

the applied voltage of alternating current. It can be seen that the oscillation amplitude of the ZnO NWs has a linear dependence on the applied voltage of alternating current.

The full width at half-maximum (fwhm) of the resonance peaks in the above two cases are determined and shown in Figure 3f and 3g. The first ZnO NW has a resonance frequency of 378.78 kHz, $\Delta f/f$ = 0.051% (f is the resonance frequency, and the mechanical quality factor $Q_1 = f_1/\Delta f_1 \approx 1972$) for a vacuum of 5×10^{-8} Torr, while the second one has a resonance frequency of 437.65 kHz, $\Delta f/f$ = 0.087% ($Q_2 = f_2/\Delta f_2 \approx 1153$). The amplitude and frequency approximately accord with Lorentzian relationship, as expected for damped harmonic vibrations.

For engineering materials, the cycles for fatigue tests are commonly between 10^7–10^8; here, 10^8–10^9 is chosen as the cycle cardinal number in order to measure precisely. The ZnO NWs vibrate for 8.94–16.81 $\times$ 10^8 cycles in 36–64 min and have no damage or failure produced that can be seen in the inset of Figure 3d. While the amplitude of the ZnO NW decreases as time grows due to the damping effect. The amplitudes of the four tests as function of time and vibration cycles are shown in Figure 3h,i, respectively. The amplitude exhibits an exponential decay with time or vibration cycles increasing. The four plots of the amplitude versus time can be fitted by the following equations (the equations in terms of the amplitude and vibration cycles are omitted here since they are similar to the eqs 4–7)

$$A_{11} = 1.981 \times \exp\left(\frac{-t_{11}}{822.770}\right) + 0.131 \quad (4)$$

$$A_{12} = 2.412 \times \exp\left(\frac{-t_{12}}{1123.914}\right) + 0.062 \quad (5)$$

$$A_{21} = 1.147 \times \exp\left(\frac{-t_{21}}{1000.039}\right) + 0.204 \quad (6)$$

dx.doi.org/10.1021/nl403426c | Nano Lett. 2014, 14, 480–485

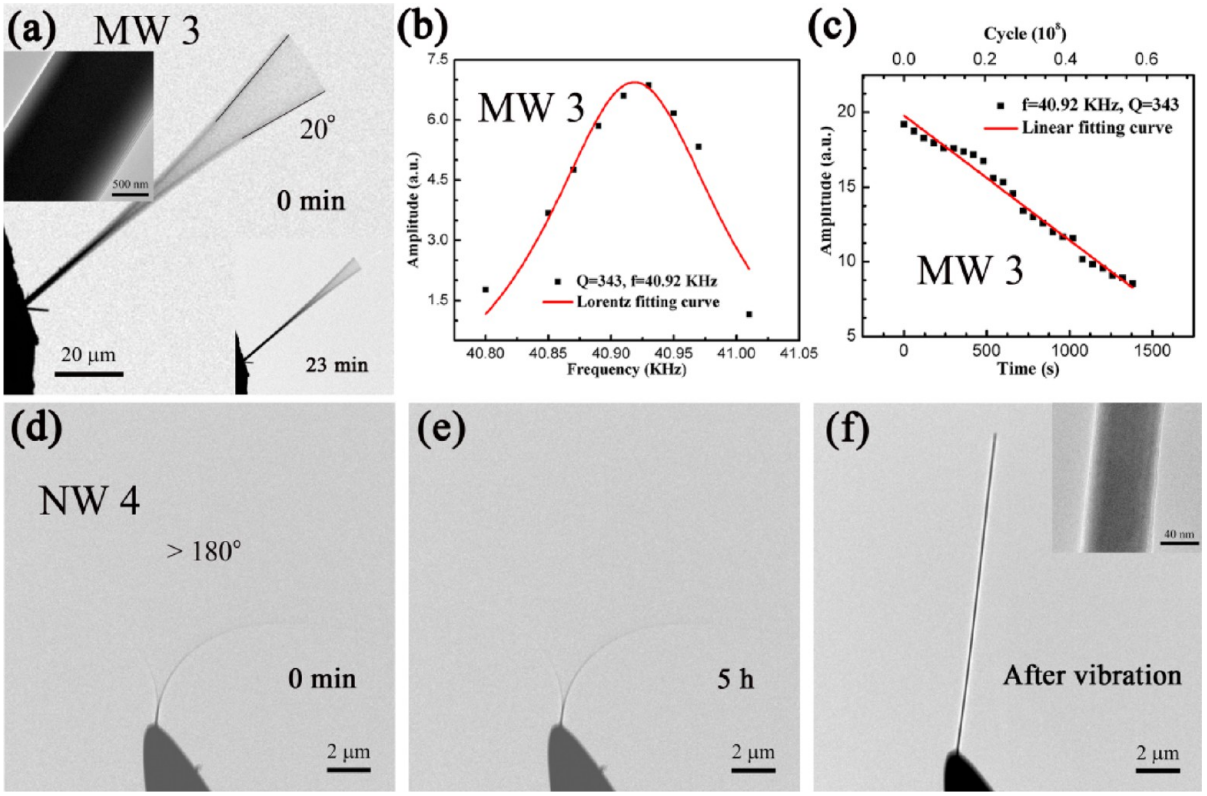

Figure 4. (a) In situ TEM resonance images of the ZnO MW with d_3 = 1596 nm: A_3 = 19.189 μm. (b) The measured fwhm of the resonance peaks. (c) The relationship between the amplitude of the ZnO MW and time/cycles. (d–f) In situ TEM resonance images of the 70 nm ZnO NW with larger amplitude in various states.

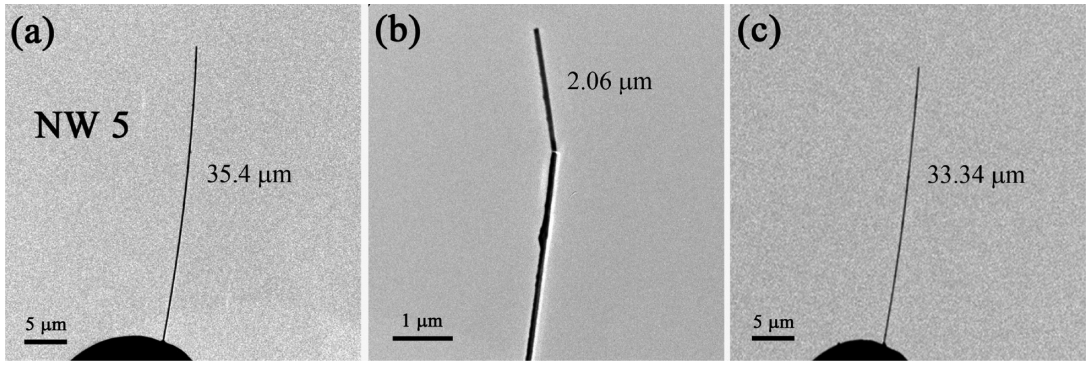

Figure 5. TEM images of a ZnO NW with d_5 = 95 nm: (a) original, (b) damaged after e-beam irradiation, (c) fractured after resonance for seconds.

$$A_{22} = 2.737 \times \exp\left(\frac{-t_{22}}{809.002}\right) + 0.366 \quad (7)$$

To further illustrate the effects of diameter and length on the fatigue behavior of ZnO wires, another two wires were investigated. Figure 4a shows in situ TEM resonance images of the third ZnO microwire (MW) with l_3 = 110.3 μm and d_3 = 1596 nm. The oscillation amplitude of the ZnO MW is A_3 = 19.189 μm, corresponding to a vibration angle of 20° ($\varepsilon_3 = d_3/2R_3$ = 1596/(2 × 171101) = 0.47%). After vibrating for 0.56 × 10^8 cycles in 23 min, no damage or failure occurs (see the inset of Figure 4a). Figure 4b shows the fwhm of the resonance peak of the ZnO MW with a resonance frequency of 40.92 kHz, $\Delta f/f$ = 0.292% ($Q_3 = f_3/\Delta f_3 \approx 343$), and the amplitude and frequency also approximately accord with Lorentzian relationship. The amplitude decay curve of the ZnO MW with time and vibration cycles is shown in Figure 4c. Unlike the amplitude exponential decay mode of the ZnO NW in Figure 3h,i, the amplitude of the ZnO MW has an approximate linear decay, which may be ascribed to the huge internal friction of the ZnO MW. In addition, a larger amplitude is adopted to measure the fourth ZnO NW with l_4 = 14.5 μm and d_4 = 70 nm (Figure 4d–f). Even with a vibration angle more than 180° ($\varepsilon_4 = d_4/2R_4$ = 70/(2 × 2200) = 1.59%, the calculation data taken from the root of the ZnO NW), no damage or failure occurs for 47.41 × 10^8 cycles in 5 h.

Aside from the influence of size, amplitude, vibrating time, and cycles on the fatigue behavior of ZnO wires discussed above, unexpected environmental factor like e-beam irradiation is also considered. The ZnO NW with l_5 = 35.4 μm and d_5 = 95 nm was irradiated by the e-beam for 10 min before the resonance. The damaged ZnO NW fractured after resonance for seconds. The morphologies of the original, damaged, and

dx.doi.org/10.1021/nl403426c | Nano Lett. 2014, 14, 480–485

fractured ZnO NW are shown in Figure 5a–c. The results indicate that intact ZnO wires have infinite fatigue life (the vibration number is more than 10^9) to bear high-cycle vibration, while the damaged ZnO NWs have very low fatigue life.

As for the fracture mechanisms of the ZnO wires, melting induced by Joule heat[28] and overstress or local stress concentration[29] have been proposed. In our case, the applied strains during the electromechanical resonance tests are on small level ($\varepsilon < 5\%$), and the stress is uniformly distributed all over the whole wire. As a result, the ZnO wire is in small stress-state, which prevents it from fracture or failure. Instead of uniform stress or strain, the damaged ZnO NW possesses local stress concentration induced by e-beam irradiation, which leads to the fracture during electromechanical resonance tests.

From the fitted curves of amplitude versus resonance frequency, the elastic modulus of the ZnO wires can be determined easily. According to the classical elasticity theory, the fundamental resonance frequency[4] is

$$f_i = \frac{\beta_i^2 D}{8\pi L^2 \left(\frac{E}{\rho}\right)^{1/2}} \tag{8}$$

Therefore, the elastic bending modulus is given by

$$E = \rho \left[\frac{8\pi f_i L^2}{\beta_i^2 D}\right]^2 \tag{9}$$

where β_i is a constant for the ith harmonic, $\beta_1 = 1.875$ and $\beta_2 = 4.694$, E is the elastic bending modulus of the ZnO wire, L is the length of the ZnO wire, D is the diameter of the ZnO wire, and ρ is the mass density. The lengths and diameters of the ZnO wires can be measured through the TEM images. The size values and calculated mechanical parameters are summarized in Table 1. The elastic bending moduli of the five ZnO wires

Table 1. The Geometrical and Mechanical Parameters of the ZnO Wires

no.	times	L (μm)	D (nm)	f (kHz)	A (μm)	E (GPa)	cycles (10^8)
1	1	9.735	148	378.78	2.000	16.8	8.94
1	2	9.735	148	378.78	2.340	16.8	9.01
2	1	9.912	177	437.65	1.319	16.9	9.54
2	2	9.912	177	437.65	3.064	16.9	16.81
3	1	110.3	1596	40.92	19.189	27.8	0.56
4	1	14.5	70	263.40	larger	179.1	47.41
5	1	35.4	95	51.00		129.5	

are 16.8, 16.9, 27.8, 179.1, and 129.5 GPa. The relationship between the modulus and the diameters is shown in Figure 6. It can be seen that the modulus of the ZnO NWs with diameters less than 100 nm approaches or exceeds the bulk modulus 140 GPa, while the modulus of the ZnO wires with diameters more than 100 nm is far below that of the bulk ZnO.

Conclusions. In summary, the investigation of fatigue behavior of ZnO wires under high-cycle strain was performed with in situ TEM electromechanical resonance method. The modulus of the ZnO NWs with diameters less than 100 nm approaches or exceeds the bulk modulus 140 GPa, while the modulus of the ZnO wires with diameters more than 100 nm is far below that of the bulk ZnO. No damage or failure was observed in the intact ZnO wires after resonance for about 10^8–10^9 cycles, while the damaged ZnO NW subjected to

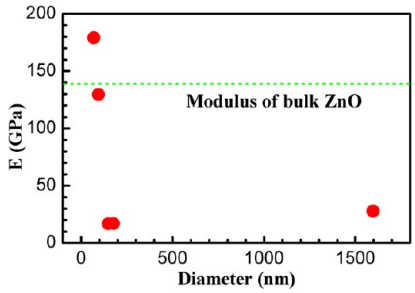

Figure 6. Young's modulus of the ZnO wires with different diameters.

e-beam irradiation fractured after resonance for seconds. The research results will provide a useful guide for designing, fabricating, and optimizing electromechanical nanodevices based on ZnO nanomaterials, as well as future applications..

Experimental Section. ZnO wires were synthesized by chemical vapor deposition (CVD) that was introduced in detail in our previous works.[4,5] The lengths and diameters of the ZnO wires are in the range of 5–120 μm and 100–2000 nm, respectively.

In this Letter, the fatigue behavior of ZnO wires was investigated by means of in situ TEM technique based on the electric-field-induced resonance.[26,30,31] The load cycles can be applied to the ZnO wire by a periodic electrostatic force driven at the ZnO wire's resonance frequency. To carry out the fatigue behavior measurements of ZnO wires, a specimen holder for a JEOL-2010 HRTEM (200 kV) was built for applying a voltage of alternative current across the ZnO wire and its counter electrode. The specimen holder has two electrodes and a set of piezomanipulation and translation devices. One end of the ZnO wires was attached to an electrochemically etched tungsten (W) tip with tip diameter of ~200 nm by a dielectrophoresis method. The other end was set free and pointed to the counter electrode, a gold (Au) ball with diameter of 0.1 mm. Then the ZnO wire was fixed on the W tip tightly enough by the amorphous carbon deposition.

To accurately measure the length and diameter of the investigated ZnO wire, the specimen holder could be rotated about its axis so that the ZnO wire and the vibrating plane could be aligned perpendicular to the e-beam. An oscillating voltage with tunable frequency was applied across the two electrodes. Because the electric induced charge on the tip of the ZnO wire oscillates at the frequency of the applied voltage of alternative current, thus, electromechanical resonance is induced if the applied frequency matches the natural vibration frequency. The ZnO wire vibrates with large amplitude in the resonance state. The resonance is directly viewed on the TV screen attached to the TEM and recorded by a charge-coupled device camera. During the loading processes, quick view was taken to see if the ZnO wire had been resonating at the amplitude and if fracture had occurred.

AUTHOR INFORMATION

Corresponding Author

*E-mail: yuezhang@ustb.edu.cn.

Notes

The authors declare no competing financial interest.

#These authors contributed equally to this work.

ACKNOWLEDGMENTS

This work was supported by the Program of Introducing Talents of Discipline to Universities, the National Major Research

Program of China (2013CB932602), the Program of International S&T Cooperation (2012DFA50990), NSFC (51372020, 51232001, 51002008, 51172022), the Research Fund of Co-construction Program from Beijing Municipal Commission of Education, the Fundamental Research Funds for the Central Universities, Program for Changjiang Scholars, and Innovative Research Team in University.

REFERENCES

(1) Wang, Z. L.; Song, J. H. Piezoelectric nanogenerators based on zinc oxide nanowire arrays. *Science* **2006**, *312*, 242−246.
(2) Wang, X. D.; Summers, C. J.; Wang, Z. L. Large-Scale Hexagonal-Patterned Growth of Aligned ZnO Nanorods for Nano-Optoelectronics and Nanosensor Arrays. *Nano Lett.* **2004**, *4*, 423−426.
(3) Wang, X.; Zhou, J.; Song, J.; Liu, J.; Xu, N.; Wang, Z. L. Piezoelectric Field Effect Transistor and Nanoforce Sensor Based on a Single ZnO Nanowire. *Nano Lett.* **2006**, *6*, 2768−2772.
(4) Huang, Y. H.; Bai, X. D.; Zhang, Y. *In situ* mechanical properties of individual ZnO nanowires and the mass measurement of nanoparticles. *J. Phys.: Condens. Matter* **2006**, *18*, 179−184.
(5) Huang, Y. H.; Zhang, Y.; Gu, Y. S.; Bai, X. D.; Qi, J. J.; Liao, Q. L.; Liu, J. Field Emission of a Single In-Doped ZnO Nanowire. *J. Phys. Chem. C* **2007**, *111*, 9039−9043.
(6) Yang, R. S.; Qin, Y.; Li, C.; Zhu, G.; Wang, Z. L. Converting Biomechanical Energy into Electricity by a Muscle-Movement-Driven Nanogenerator. *Nano Lett.* **2009**, *9*, 1201−1205.
(7) Lu, M. P.; Song, J. H.; Lu, M. Y.; Chen, M. T.; Gao, Y. F.; Chen, L. J.; Wang, Z. L. Piezoelectric Nanogenerator Using p-Type ZnO Nanowire Arrays. *Nano Lett.* **2009**, *9*, 1223−1227.
(8) Wang, Z. L. Nanopiezotronics. *Adv. Mater.* **2007**, *19*, 889−892.
(9) He, J. H.; Hsin, C. L.; Liu, J.; Chen, L. J.; Wang, Z. L. Piezoelectric gated diode of a single ZnO nanowire. *Adv. Mater.* **2007**, *19*, 781−784.
(10) Zhou, J.; Gu, Y. D.; Fei, P.; Mai, W. J.; Gao, Y. F.; Yang, R. S.; Bao, G.; Wang, Z. L. Piezoelectric-Potential-Controlled Polarity-Reversible Schottky Diodes and Switches of ZnO Wires. *Nano Lett.* **2008**, *8*, 3973−3977.
(11) Zhou, J.; Gu, Y. D.; Fei, P.; Mai, W. J.; Gao, Y. F.; Yang, R. S.; Bao, G.; Wang, Z. L. Flexible Piezotronic Strain Sensor. *Nano Lett.* **2008**, *8*, 3035−3040.
(12) Chen, C. Q.; Zhu, J. Bending strength and flexibility of ZnO nanowires. *Appl. Phys. Lett.* **2007**, *90*, 043105.
(13) Hoffmann, S.; Ostlund, F.; Michler, J.; Fan, H. J.; Zacharias, M.; Christiansen, S. H.; Ballif, C. Fracture strength and Young's modulus of ZnO nanowires. *Nanotechnology* **2007**, *18*, 205503.
(14) Xu, F.; Qin, Q. Q.; Mishra, A.; Gu, Y.; Zhu, Yong. Mechanical properties of ZnO nanowires under different loading modes. *Nano Res.* **2010**, *3*, 271−280.
(15) Agrawal, R.; Peng, B.; Gdoutos, E. E.; Espinosa, H. D. Elasticity Size Effects in ZnO Nanowires−−A Combined Experimental-Computational Approach. *Nano Lett.* **2008**, *8*, 3668−3674.
(16) Agrawal, R.; Peng, B.; Espinosa, H. D. Experimental-computational investigation of ZnO nanowires strength and fracture. *Nano Lett.* **2009**, *9*, 4177−4183.
(17) Gao, P. X.; Mai, W. J.; Wang, Z. L. Superelasticity and Nanofracture Mechanics of ZnO Nanohelices. *Nano Lett.* **2006**, *6*, 2536−2543.
(18) Ni, H.; Li, X. D. Young's modulus of ZnO nanobelts measured using atomic force microscopy and nanoindentation techniques. *Nanotechnology* **2006**, *17*, 3591−3597.
(19) Wen, B. M.; Sader, J. E.; Boland, J. J. Mechanical properties of ZnO nanowires. *Phys. Rev. Lett.* **2008**, *101*, 175502.
(20) Jing, G. Y.; Zhang, X. Z.; Yu, D. P. Effect of surface morphology on the mechanical properties of ZnO nanowires. *Appl. Phys. A: Mater. Sci. Process.* **2010**, *100*, 473−478.
(21) Yang, Y.; Qi, J. J.; Gu, Y. S.; Guo, W.; Zhang, Y. Electrical and mechanical coupling nanodamage in single ZnO nanobelts. *Appl. Phys. Lett.* **2010**, *96*, 123103.
(22) Zhang, Y.; Yan, X. Q.; Yang, Y.; Huang, Y. H.; Liao, Q. L.; Qi, J. J. Scanning probe study on the piezotronic effect in ZnO nanomaterials and nanodevices. *Adv. Mater.* **2012**, *24*, 4647−4655.
(23) Gao, Z. Y.; Ding, Y.; Lin, S. S.; Hao, Y.; Wang, Z. L. Dynamic fatigue studies of ZnO nanowires by in-situ transmission electron microscopy. *Phys. Status Solidi RRL* **2009**, *3*, 260−262.
(24) Bai, X. D.; Wang, E. G.; Gao, P. X.; Wang, Z. L. Measuring the Work Function at a Nanobelt Tip and at a Nanoparticle Surface. *Nano Lett.* **2003**, *3*, 1147−1150.
(25) Gao, R. P.; Pan, Z. W.; Wang, Z. L. Work function at the tips of multiwalled carbon nanotubes. *Appl. Phys. Lett.* **2001**, *78*, 1757−1759.
(26) Poncharal, P.; Wang, Z. L.; Ugarte, D.; Heer, W. A. Electrostatic deflections and electromechanical resonances of carbon nanotubes. *Science* **1999**, *283*, 1513−1516.
(27) Xu, S. G.; Guo, W. H.; Du, S. W.; Loy, M. M.; Wang, N. Piezotronic Effects on the Optical Properties of ZnO Nanowires. *Nano Lett.* **2012**, *12*, 5802−5807.
(28) Zhang, Q.; Qi, J. J.; Yang, Y.; Huang, Y. H.; Li, X.; Zhang, Y. Electrical breakdown of ZnO nanowires in metal-semiconductor-metal structure. *Appl. Phys. Lett.* **2010**, *96*, 253112.
(29) Li, P. F.; Huang, Y. H.; Wang, Z. Z.; Lu, S. N.; Yan, X. Q.; Liao, Q. L.; Zhang, Y. Probing of electrical, mechanical, and electro-mechanical coupling effects on single ZnO nanobelts by C-AFM testing system. Unpublished work, 2013.
(30) Bai, X. D.; Gao, P. X.; Wang, Z. L.; Wang, E. G. Dual-mode mechanical resonance of individual ZnO nanobelts. *Appl. Phys. Lett.* **2003**, *82*, 4806−4808.
(31) Huang, Y. H.; Zhang, Y.; Wang, X. Q.; Bai, X. D.; Gu, Y. S.; Yan, X. Q.; Liao, Q. L.; Qi, J. J.; Liu, J. Size Independence and doping dependence of bending modulus in ZnO nanowires. *Cryst. Growth Des.* **2009**, *9*, 1640−1642.